

Performance of scientific tractography for presurgical preparation of area seizing abrasions: A study through the acquisition plus post-processing techniques contrasted to investigational revisions

V Rama Raju^{1*}

¹Professor, ¹CMR College of Engineering & Technology, Kandlakoya, Medchal Rd., Hyderabad, Telangana, India

***Corresponding Author: V Rama Raju**

Email-id: drvrr@cmrcet.org

Abstract

There is limited (consistency) normalization of acquisition and processing methods in diffusion tractography for presurgical development, managing to a range of methodologies. This study investigated the number of representative acquisition variants and post processing techniques are deemed, to evaluate their significance while applying a scientific tractography system programme. Magnetic resonance imaging (M.R.I., i.e., the diffusion-MRI) was commenced in normal controls, utilizing protocols classic of scientific and research scanning: a 32direction-diffusion-acquisition (Dir-DA) in conjunction with and devoid of peripheral-gating, and a nongated 64diffusion-direction-acquisition (Dif-DA). All the data sets were post processed by employing the diffusion-tensor-reconstruction(D.T.R) by rationalize tractography, plus thru controlled spheric deconvolution (C.S.D) via rationalize (i.e., streamline) also likelihood probabilistic-tractography, to delineate the cortico-spinal-tract (C.S.T) plus optic-radiation (O.R). The precision of tractography findings were assessed versus a histologic atlas-map by applying a unique probabilistic dice-overlap-technique (D.O.T), alongside explicit contrast to tract sizes and space of Meyer's loop to temporal pole (M.L.T.P) from analyses (dissection) observations. Tracts generated by C.S.D with likelihood-tractography supplied the maximum overlap with the histologic atlas-map (overlap-scores of 45% and 53% for CST plus OR) and top matched tract-volume and M.L.T.P gap through dissections. The acquisition protocols examined experimentally had some degree of effect on the exactitude-of-tractography. In all subjects, the C.S.D based likelihood tractography generated tracts with most structural acceptability, while in one case structurally reasonable pathways might not be modernized or restored devoid of lowering the probabilistic-threshold, foremost to a rise in erroneous false-+Ve (positive)tracts. Innovative and sophisticated post processing techniques such as CSD with probabilistic tractography are vital for presurgical planning. But total precision virtual to separation experiments continues inadequate.

Keywords: Controlled spheric deconvolution (C.S.D), Diffusion MRI, tractography, Probabilistic dice-overlap-technique (D.O.T), Cortico-spinal-tract (C.S.T)

Introduction

The application of diffusion imaging based tractography to advise, notify and update and direct and then point the invasive, i.e., surgical-operation resection of space inhabiting and then seizing (or occupying) the lesions is turn out to be progressively predominant. And the main reason is because of the addition of scientific research technical and technological innovative engineering medical computer programme (the software) into experimental neuro surgical-planning-systems. At the beginning, in the early hours, it was known that tractography is inadequate and restricted in entirely illustrating the fundamental and inherent anatomical-structure,¹ which can in part be accredited, ascribed, and attributed too to a few technical challenges.²⁻³ One such constraint, one such restriction registered and stated in the literature is the interruption to the tracking-process which can ensue as a result of signal-loss in diffusion-weighted-images(D.W.Is) from vascular and C.S.F-pulsation.⁴⁻⁵ To prevent this object, groups have indicated that peripheral-tangential-gating(P.T.G) the recording of D.W.I images acquisition to the cardiac-cycle ought to be embark on. Though, there has been partial execution and performance of this in the experimental-clinical and scientific-setting due to increase in intensity in grep or search-time, i.e., time-of-scanning and complexities and intricacies in the subject (patient)-planning.² One more issue of tractography is the incapacity to illustrate all grey-matter estimates quite-

absolutely in areas of complicated and dense-fiber structural-design. The greenest form of tractography based on the diffusion-tensor/DT-model presumes just and merely a specific fiber population inside a voxel, however it has been demonstrated greater than 91% of the gray-matter voxels in a characteristic-D.W.I-images gathering will encompass as a minimum in any case 2-fiber subjects.⁶ Despite this, the experimentally existing tractography-systems appear to solely achieve D.T-based-tractography. Procedures to improve and explicate and clarify the complex-fiber architectural-design have been existing in the scientific-research and technical-setting for some time and also incorporate methodologies which paradigm criss-crossing fiber design⁷⁻¹¹ and likelihood-probabilistic tractography.¹² Numerous studies have emphasized the requirement for experimentally medical-based-systems to execute this sophisticated diffusion-processing-approach.¹³⁻¹⁴

But, to execute productively these sophisticated techniques a comprehensive and detailed knowledge and interpretation is necessary for the further procurement gathering needs plus processing-parameters linked through the additional complicated development-modelling. One such variable is the maximum-threshold-limit in probabilistic tractography; altering this level strongly impacts the number of the false+Ve-positive and false-Ve-negative pathways incorporated in the final-tract interpretation.¹⁵⁻¹⁷ One more issue which has been broadly examined in the literature

reflects the number of diffusions-encoding-directions mandatory for tractography. This ideal number has been explored in various-settings comprising through the duplicability of quantifiable-system-of-measurements(the-“metrics”)¹⁸ the precision of structural-representation¹⁹ and in the context of different diffusion modelling algorithms.²⁰ The literature supports differing-analyses on the ideal number-of-routes, creating it complicated for a experimental-medical-site executing tractography, to know, which protocol-exemplifies the greatest agreement amongst data-quality and the time-of-grep (“grep-time”). In conjunction with numerous apparently ostensibly significant technical and technological enhancements in diffusion-gathering and tractography-processing it can be able to frequently be intimidating for an inexperienced user to know-how-best to pledge a database-of-tractography for neuro surgical-planning. Integrating all the indicated modifications be able to make possible longer grep-times plus the condition for specialized technical-and-technological and procedural-knowledge in gain-setup and offline-processing wherein only inbuilt functions. In this connection, the purpose of the study stated here was to explore these contrasting approaches as well as evaluate their importance in experimental-medical particularly tractography of the cortico-spinal-tract(CST) plus optic-radiations(O.R) for neuro surgical-planning of space-occupying lesions (S.O.Ls). With this application in mind, the objective is to address the some of the issues mentioned below:

1. In what way tractography is induced by the number of diffusions encoding paths gathered
2. In what manner tractography is inspired by the usage of tangential gating
3. Whether and by what means the outcomes of sophisticated processing-techniques, incorporating constricted-spheric-deconvolution(C.S.D) and probabilistic tractography, differ from DTI based methods with streamline tractography, as implemented as standard on our neurosurgical planning system and

Subject	Age	Gender	Diagnosis
1	15	M	Right peri-Rolandic Ganglioglioma WHO-grade-I
2	58	M	Left frontal Oligodendroglioma WHO-grade-II
3	51	F	Left parietal arterial venous malformation (AVM)

Data gathering

The magnetic resonance imaging was executed using a 1.5T-HDxt system with an 8-channel head coil. Anatomical-structural MRI-images were gathered together with a 3D-IR prepared-spoiled-gradient-echo-sequence (IRSPGR); TI=300ms, TE=5ms, TR=11.6ms, Flip-angle=20, FOV=28cm, 131 slice-locations, 1.1mm isotropic-voxel-size, ASSET (parallel imaging) factor=2. The DWI-asset developed a two-fold/double refocused/transferred spin-echo EPI-sequence; TR=17s, TE=101ms. This “ground” procurement was subsequently repetitive later with the following modifications applied separately: (a) 64 diffusion directions with 7 b = 0 images (acquisition time, 20min 02s); (b) peripheral gating to the cardiac cycle with effective TR =

4. What the optimal threshold is for probabilistic based tractography in applications such as these. The purpose of this investigation was to understand where best to focus our efforts, such that an optimal tractography acquisition and processing pipeline could be implemented within our clinical setting.

All of the above methodologies have been investigated and reported previously in various settings. The novel aspect of our work is to assess the tractography results against the Ju'lich histological-atlas²¹ using a probabilistic Dice overlap technique²² and through a direct comparison between tract volumes and anatomical location with equivalent measures reported in dissections studies.²³⁻²⁵ We use this assessment to determine an optimum acquisition and processing protocol. The fuzzy Dice overlap technique has never previously been used as a metric for assessment of tractography accuracy and to the best of our knowledge dissection studies have only previously been evaluated against the OR. By comparing to a few dissection metrics for both the CST and OR we provide the most comprehensive body of work comparing tractography methods to dissection studies for application to neurosurgical planning.

Finally we show the result of applying our suggested optimized processing protocol to a series of clinical case studies.

Material and Methods

10 normal control young subjects were involved in the study. Subjects informed consent (written) was attained with approval from the institute ethical committee following the Helsinki principles. Data from three patients referred to the neurosurgical unit at our tertiary care unit for presurgical imaging were also included retrospectively as part of a clinical audit undertaken according to CMR Hospital standard policies and procedures (Table 1) Subjects characteristics

15 R-R intervals (10min 48s). This gave a total of three raw diffusion acquisition data sets which are subsequently labelled; 32 dir (for the 32 direction acquisition), 64 dir (for the 64 direction acquisition) and 32 dir PG (for the 32 direction acquisition with peripheral gating). The decision to test 32 and 64 direction diffusion acquisition schemes was in part motivated by the work of²⁰ who suggests that 45 directions is the minimum to be used for processing methods which attempt to reconstruct multiple fiber populations within a voxel. Despite this, groups have successfully investigated diffusion tractography based on reconstruction algorithms that identify multiple fiber populations within a voxel for neurosurgical planning with diffusion encoding schemes of < 45 directions²⁶⁻²⁸ It has also been shown for DTI

that at least 30 unique sampling orientations are required for a robust estimation of the tensor orientation.¹⁸ Given these results, we opted to test a 32 direction encoding scheme (having a clinically acceptable acquisition time of 10 min) against a 64 direction encoding scheme, chosen to be consistent with reports of similarly high numbers of encoding directions.^{14,29-30} Given the increased imaging time for the 64 direction acquisition (>20mins) a strong justification of additional utility would be required for us to implement in our clinical population.

Diffusion processing

Raw diffusion data were initially viewed in cine mode using fslview (www.fmrib.ox.ac.uk/fsl/fslview) and it was found there was limited motion present. Retrospective motion correction could have been applied via tools incorporated into the different processing methods investigated in this study (methods described below). However, the motion correction techniques differed for each method and therefore for consistency, and since limited motion was present in our data, no correction was applied.

Each diffusion data set was post-processed using the CE marked StealthViz tractography processing software (Medtronic, Colorado, USA) which utilizes a diffusion tensor reconstruction and the FACT streamline tractography algorithm.³¹ The raw diffusion data was subsequently taken offline and processed using the MRTrix software package (www.mrtrix.org).

Tracts were produced using the constrained spherical deconvolution (CSD) reconstruction, with tractography subsequently implemented based on the streamline and bootstrap probabilistic algorithms.³²

For the cortico-spinal tract a seed region was defined within the posterior limb of the internal capsule (PLIC), including only those voxels with diffusion predominantly in an inferior/superior direction as identified blue/purple on a colour coded fractional anisotropy map (Fig 1).³³

For the optic radiation two seed regions were defined using the method described by.³⁴ The first contained voxels which were antero-lateral to the lateral geniculate nucleus (LGN) at the base of the Meyer's loop with diffusion directions predominantly in an antero-medial to posterolateral orientation (Fig 1B(ii)). The second was in the section of the Meyer's loop (Fig 1B(i)). A waypoint was defined in the lateral wall of the occipital horn of the lateral ventricle at the posterior extent of the corpus callosum (Fig 1 B(iii)). Using these ROI's alone often results in the optic radiation including tracts from the inferior longitudinal fasciculus. To remove these erroneous pathways an objective, iterative process was performed on the tracts produced by CSD-based probabilistic tractography. The process involved moving an exclusion mask posteriorly until it began to coincide with the Myers loop, leading to thinning of the optic radiation. The final location for the exclusion mask was chosen when 90% of the original tract volume remained, as determined through calculating the number of voxels in the resultant tract image. The tractography undertaken with this "90%" exclusion mask applied was assumed to be the best representation of the optic

radiation. This exclusion mask was then applied to the tractography obtained from the other processing methods (as discussed below).

Seed and waypoint ROI's definition files were copied from the STEALTH workstation ensuring that identical regions were used between the STEALTH and MRTrix-based processing. Therefore, any differences in tractograms could be attributed to the processing method rather than differences in ROI location.

The tractography process was terminated when streamlines entered voxels with a fractional anisotropy (FA) < 0.1 for DTI-based streamline tractography, with a fiber orientation distribution (FOD) amplitude < 0.1 for CSD-based streamline tractography, and an FOD amplitude < 0

for the CSD-based probabilistic tractography. The FA threshold in this study was set to 0.1 to ensure tractography was not prematurely terminated in regions of peritumoural oedema. For all tractography processing the maximum curvature was set to 450 for the corticospinal tract (the default curvature setting for the StealthViz package) but was increased to 1800 for tractography of the optic radiation to ensure the high curvature tracts within the Meyer's loop were not removed. Tractography step size for all algorithms was set at 1mm. In StealthViz the 3D object distance parameter was set to zero to ensure there was no artificial inflation of the tract volume.

For probabilistic tractography the output is a probability map with image intensities that corresponds to the number of streamlines passing through each voxel normalised to the total number of streamlines generated. These maps were thresholded such that voxels with probabilities less than 0.005, 0.01, 0.025, 0.05 and 0.075 had their value set to zero, and subsequently a binary map was created in NIFTI format for each threshold. Tractography outputs from the streamline methods were also converted to binary images, in which all voxels that were intersected by a streamline were considered to be part of that tract.

In total seven binary tract images were created corresponding to each processing method. These methods have been labelled as: (1) STEALTH (for DTI-based streamline tractography generated using the StealthViz package), (2) CSD-stream (for CSD reconstruction with streamline tractography generated using MRTrix), (3) Prob 0.005, (4) Prob 0.01, (5) Prob 0.025, (6) Prob 0.05 and (7) Prob 0.075 (for CSD reconstruction with probabilistic tractogra-

phy generated using MRTrix, thresholded at 0.005, 0.01, 0.025, 0.05 and 0.075, respectively).

CST Tractography

In addition, a "sub-study" was undertaken on a limited dataset with the aim of identifying if the inclusion of a waypoint ROI improved the tractography of the CST. The analysis was undertaken on the 32dir data (as it was expected that the outcome would not be overly dataset dependent) for the CSD-based probabilistic tractography processing using the PLIC seed ROI described above (Fig 1A) and a waypoint region placed in the precentral gyrus (Figure 2). Tracts were

only included in the final probability map if they intersected this waypoint region.

Evaluation of tract

Standard space. For the volunteer subjects, the diffusion images were aligned to their structural images using `epi_reg` (www.fmrib.ox.ac.uk/fsl/FLIRT) and the structural images were aligned to the Colin27T1 atlas using FNIRT (www.fmrib.ox.ac.uk/fsl/fnirt). The combined warp from `epi_reg` and FNIRT was then applied to the binary tract images, aligning these to the Colin27T1 atlas. The tracts were then summed for all 10 subjects to create a tract probability map. The tract probability map was compared to the Ju'lich atlas which is aligned to the same Colin27T1 atlas. The Ju'lich atlas consists of cytoarchitectonic maps of the white matter structures in the brain obtained from dissection studies.²¹ The intensity of the voxels within these maps represents the probability that the voxel contains a particular tract based on 10 subjects. Comparisons with the Ju'lich atlas were performed both qualitatively, through visual inspection, and quantitatively by calculating the fuzzy Dice overlap scores.²² The fuzzy Dice overlap quantifies the overlap of non-binary images whose voxel intensities vary across a fixed range, giving an overlap score in the range.¹ In our case the two inputs were the combined subject tract probability map and the probability maps from the Ju'lich atlas.

Native space. The tract volume of the CST and OR for each subject was determined in their native space by summing the number of voxel in the binary tract image and multiplying by the voxel size. The Meyer's loop to temporal pole (ML-TP) distance was measured for the OR only, and was determined from the difference in the anterior-posterior coordinate between the most anterior tip of the Meyer's loop, (identified from tractography) and temporal pole as identified visually on the non-diffusion-weighted ($b = 0$) image. The accuracy of the ML-TP distance and the tract volume for the different methods was assessed by comparing to equivalent data obtained from published dissection studies.^{24-25,35-36}

Statistical analysis. The data sets for tract volumes and ML-TP distance across the 10 volunteer subjects were tested for normality using the Shapiro-Wilks test. All data demonstrated a normal distribution and subsequently a one-way ANOVA investigation was undertaken to determine if the data could be considered to all be drawn from the same distribution. In cases where the data failed the ANOVA null hypothesis, a post-hoc Tukey honest significant difference (HSD) analysis was undertaken. Significance levels for all statistical testing was set to 0.05 and analysis was undertaken using MATLAB (Boston, USA).

Studies through scientific

The investigation in our volunteer cohort suggested (see results section below) that the 64 direction acquisition and peripheral gating had limited impact on the quality of tractography. For our patient cohort we therefore implemented the 32 direction acquisition protocol. A qualitative comparison was undertaken comparing all seven processing methods. The fuzzy DICE overlap, ML-TP and

tract volume measurements were not applied in the patient cohort since tissue distortion from the lesions would lead to expected misalignment with the atlas/dissection results.

Results and Discussion

Tracts were successfully depicted the CST in all subjects for all acquisition and post processing methods investigated. For the OR the CSD reconstruction with probabilistic tractography successfully depicted the pathway in all hemispheres. In 6 hemispheres CSD-based streamline tractography did not generate any tracts to depict the OR and in 4 hemispheres the DTI-based streamline tractography did not generate any tracts. This occurred for the 32 direction acquisition (1 hemisphere) and the 64 direction acquisition (3 hemispheres). These null results were included in fuzzy Dice overlap, and volume analysis but excluded from the analysis of the average ML-TP distance.

Dice overlap measure. Results for the fuzzy Dice overlap analysis are shown in Fig 3, demonstrating only small differences in overlap between the tracts generated from the various acquisition protocols. Differences in overlap were more apparent between processing methods. It was found when averaging the overlap results from all 3 acquisitions that the CSD-based probabilistic tractography thresholded at 0.025 and 0.05 had the greatest overlap value (44% for the CST and 50% for the OR). When considering the three different processing methodologies (DTI-based streamline, CSD-based streamline and CSD-based Probabilistic at the optimal threshold) DTI-based streamline tractography generated by StealthViz had the poorest overlap with the Ju'lich atlas for both the CST and OR (38% and 44% respectively).

Qualitative comparison. Tract frequency maps for the CST and the OR are shown in Fig 4 and Fig 5 respectively, together with the Ju'lich atlas in standard space. The results are shown comparing processing methods only, since the overlap analysis highlighted that acquisition scheme had limited impact on tractography outcome (Fig 3). In all cases increasing the probabilistic threshold decreased the core thickness together with the total length of the depicted tract. However, the core tract thickness was typically overestimated by tractography in all methods relative to the size found in the Ju'lich atlas (see white arrows in Fig 4 and Fig 5).

Areas where tractography was limited in correctly depicting the underlying anatomy included the lateral projections of the CST (see black arrows Fig 4) and the anterior projections onto the calcarine fissure (indicated by black arrows on Fig 5).

Clinical studies

Patient#1. Fig.1 indicates the results for patient 1. In the STEALTH tractography it can be seen that the lateral projections are not represented to the region of the precentral gyrus controlling hand function. They are; however represented for tractography based on the CSD reconstruction. For CSD-based probabilistic tractography at thresholds of 0.005 and 0.01 the lateral projections are well

depicted; however, the core of the CST is possibly over-represented as was the case in the volunteer cohort (Fig 4). At the optimal probabilistic threshold of 0.025 (as defined by the maximum tract overlap with the Ju"lich atlas in our volunteer cohort) the lateral projections are heavily "pruned" and at greater thresholds are no longer present.

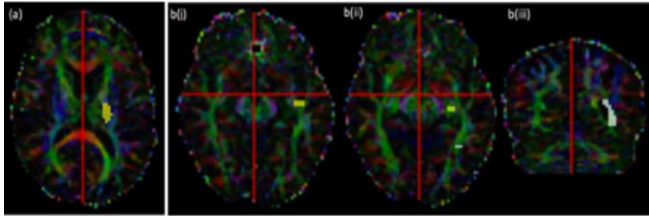


Figure 1. Informed consent subject tractography seed-R.O.I's (pale) way point R.O.I's (gray-silver) plus omission masks (reddish) for (a) C.S.T and (b) O.R@3 slice-positions.

Patient 2. For Patient 2 the lesion included significant peritumoral oedema which potentially affected the CST. The CSD-based probabilistic method for the lowest threshold of 0.005 was able to delineate nearly the entirety of the CST connecting the PLIC to all regions of the precentral gyrus (Fig 10). As the threshold was increased the connectivity to the trunk area of the pre-central gyrus dominates, and projections to the foot and the face areas are progressively removed. Probabilistic tractography at all thresholds; however, provided better delineation of the CST compared to the streamline based methods (i.e.,CSD-stream and-STEALTH).

Patient 3. For Patient 3, the CSD-based probabilistic method with a threshold less than 0.025 produced tracts depicting a fuller extent of the CST (short arrow Fig 11). However, at these low thresholds it is likely that false positive tracts are present originating at the PLIC but ending near the superior parietal lobule (long arrow Fig 11). Both sections are immediately adjacent to the AVM but only the section depicted by the shorter arrow need be considered in the context of pre-surgical planning for treatment of the A.V.M. The goal of this work was to optimize and assess the limitations of clinical tractography through a visual and quantitative comparison with dissection studies. The dissection metrics investigated included tract probability maps, tract volumes and the ML-TP distance for the optic radiation. By considering all known dissection metrics we aimed to gain the most comprehensive understanding of the accuracy of tractography in depicting the CST and OR relevant for our application of pre-surgical planning of space occupying lesions.

Conclusion

The purpose of this complex scientific study was to identify where finest, good quality, greatest and safest to concentrate endeavors in creating a vigorous clinical/experimental tractography program for presurgical planning of space inhabiting, seizing (i.e.,occupying) lesions. In this connection, we explored medically faithful variations to a usual diffusion-gathering protocol plus equated an well-known reputable and trustworthy quantifiable experimental

scientific tractography tool (Stealth-Viz) in contradiction of a M.R.Trix scientific research-discovery-tool, that is possible and practicable to contrivance and device a tool for clinical-settings.

Source of Funding

None.

Conflict of Interest

None.

References

1. M.Kinoshita,et.al.Fiber tracking does not precisely estimate size of fiber bundle in pathological condition: initial neuro surgical experience using neuro navigation and sub cortical white matter stimuli. *Neuro-imaging*.Vol.25,(2), Pp:424-9,2005.
2. P.Mukherjee,et.al.,Diffusion-tensor MR-imaging and fiber tractography:technical considerations. *AJNR-Am J Neuroradiol*. Vol.29,(5),Pp: 843-52, 2008.
3. W.I.Essayed, et.al., White-matter tracto-graphy for neuro-surgical-planning *J of Neuroimage Clin*,Vol.15,Pp:659-72.
4. D. Jones, Impact of Cardiac-Pulsation to Variability of Tractography Results. 13th Annual Meeting of the International Society of MRI in Medicine;Miami, Fla,Vol.5,Pp:234-41,2005.
5. S. Skare,On the effects of gating in diffusion imaging of the brain using single shot EPI. *MRI*.Vol.19,(8),Pp:1125-8.
6. B.Jeurissen,et.al.,Exploring the incidence of complex fiber configurations in white matter tissue with diffusion MRI. *Human Brain Mapping*.Vol.34,(11),Pp:2747-66,2013.
7. D.S.Tuch,et.al.,High angular resolution diffusion imaging reveals intravoxel white matter fiber heterogeneity.*MR Medical*.Vol. 48,(4),Pp:577-82,2002.
8. D.S.Tuch,Q-ball imaging. *Magnetic Resonance Medical*. Vol.52, (6),Pp:1358-72. 2004
9. K.M.Janson. Persistent Angular Structure: new insights from diffusion MRI data. Dummy version. *Inf Process Medical Imaging*. Vol.18,Pp: 672-83.2003.
10. J.D.Tournier,Direct estimation of the fiber orientation density function from diffusion-weighted M.R.I data using spherical deconvolution. *Neuroimaging*. Vol.23,(3),Pp:1176-85, 2004.
11. A.A.Qazi,et.al.Resolving crossings in the corticospinal tract by two-tensor streamline tractography: Method and clinical assessment using *f-MRI*. *Neuroimaging*. Vol.47,(2),Pp: 98-106,2009
12. G.J.Parker,A framework for a streamline-based probabilistic index of connectivity (P.I.Co.) using a structural interpretation of M.R.I diffusion measurements. *J MRI* Vol.18, (2), Pp: 242-54,2003.
13. S.Farquharson, et.al.White matter fiber tractography: why we need to move beyond D.T.I. *J. of Neurosurgery*, Vol.118,(6)Pp:1367-77,2013.
14. M.Bucci,et.al.,Quantifying diffusion MRI tractography of the corticospinal tract in brain tumors with deterministic and probabilistic methods. *Neuroimaging Clin*, Vol.3,Pp:361-8,2013.
15. A.T.Toosy, et.al.,Characterizing function-structure relationships in the human visual system with functional MRI and diffusion tensor imaging. *Neuroimag*. Vol.21,(4),PP:1452-64,2004.
16. P.L.Clatworthy,et.al.,Probabilistic tractography of the optic radiations—an automated method and anatomical validation.*Neuroimag*,Vol.49,No.3,Pp:2001-12,2010
17. R.Tasker et.al., The thalamus and midbrain of man. A physiological atlas using electrical stimulation. Springfield, IL: Charles C Thomas, Vol. 18, Pp: 2-9, 1982.
18. A.Fukamachi et.al.. Delineation of the thalamic nuclei with a microelectrode in stereotaxic surgery for parkinsonism and cerebral palsy. *J Neurosurg*, Vol.39,No.19, Pp:214-25,1973

19. D.Albe-Fessard,et.al..Electrophysiological detection and identification of subcortical structures in man by recording spontaneous and evoked activities. *Electroencephalogr Clin Neurophysiol*, Vol.15,(20) Pp:1052-620,1963
20. H.Narabayashi.Tremor mechanisms. In: Schaltenbrand G, Walker AE, editors. *Stereotaxy of the human brain*. Stuttgart: Georg Thieme; Vol. 2,Pp. 510–1421,1982
21. C.Bertrand,et.al.,. Stereotactic surgery for parkinsonism: microelectrode recording, stimulation, and oriented sections with a leucotome. In: Krayenbuhl H, Maspes PE, Sweet WH, editors. *Progress in neurological surgery*. Basel: Karger;Vol.22,Pp.79–112,1973
22. G.Guiot. Electrophysiological recordings in stereotaxic thalamotomy for parkinsonism. In: Krayenbuhl H, Maspes PE, Sweet WH, editors. *Progress in neurological surgery*. Basel: Karger;Vo.23,Pp.189–221,1962
23. R.Hassler.Physiological observations in stereotaxic operations in extrapyramidal motor disturbances. *Brain*; Vol. 83:Pp: 337–5024,1960
24. O.J.Andy. Sensory-motor responses from the diencephalon. Electrical stimulation in man. *J Neurosurg* Vol. 24,(3) Pp:612–20. 966
25. C.Bertrand.Functional detection with monopolar stimulation. *J Neurosurg*;Vol. 24,(3) Pp: 403, 1966
26. CW.Sem-Jacobsen, Electrical stimulation of the human brain: pitfalls and results. In: Somjen GG, editor. *Neurophysiology studied in man*. Amsterdam: *Excerpta Med*, Vol. 13, Pp. 27–36, 1972.
27. G. Schaltenbrand, et.al., *Atlas for stereotaxy of the human brain*. Stuttgart: *Georg Thieme*; Vol. 5, Pp: 31-9, 1977.
28. M. Monnier, et.al.,[Detection, stimulation and coagulation of thalamus in man]. *J Physiol* (Paris), Vol. 43, Pp: 818, 1951.
29. Ito Z. Stimulation and destruction of the prelemniscal radiation or its adjacent area in various extrapyramidal disorders. *Confin Neurol* 1975;37:41–8. 14.
30. G. L. Defer, “Core assessment program for surgical intervention therapies in Parkinson’s disease,” *Mov. Disord.* vol. 14,(4), Pp. 572–84, 1999.
31. Andrade-Souza YM, Schwalb JM, Hamani C, Eltahawy H, Hoque T, Saint-Cyr J, Lozano AM. Comparison of three methods of targeting the subthalamic nucleus for chronic stimulation in Parkinson’s disease. *Neurosurg*, vol. 62, (2), pp: 875-83, Feb 2008.
32. Larry Squire, Darwin Berg, Floyd E. Bloom, Sascha du Lac, Anirvan Ghosh Nicholas C. Spitzer, *Fundamental Neuroscience*, 4th Ed. AP Academic Press, 2012.
33. McClelland S 3rd.A cost analysis of intraoperative microelectrode recording during subthalamic stimulation for Parkinson’s disease. *Mov Disord.* 2011 Jun 14.
34. William H Press, Saul A. Teukolsky, William T. Vetterling, and Brian P. Flannery, *Numerical Recipes in C++*, Cambridge University Press, 2002.

How to cite: Raju.V R et al. Performance of scientific tractography for presurgical preparation of area seizing abrasions: A study through the acquisition plus post-processing techniques contrasted to investigational revisions *IP Int J Aesthet Health Rejuvenation* 2021;4(4):.